PCCP

PAPER

View Article Online
View Journal | View Issue

Cite this: *Phys. Chem. Chem. Phys.*, 2017, **19**, 6519

Chemical memory with states coded in light controlled oscillations of interacting Belousov–Zhabotinsky droplets

Konrad Gizynski* and Jerzy Gorecki

Received 1st November 2016,
Accepted 7th February 2017

DOI: 10.1039/c6cp07492h

rsc.li/pccp

The information storing potential of droplets, in which an oscillatory, photosensitive Belousov–Zhabotinsky (BZ) reaction proceeds, is investigated experimentally. We consider coupled oscillations in pairs and triplets of droplets. Droplets are surrounded by a solution of lipids in decane. Oscillations synchronize *via* diffusion of an activator through a lipid bilayer. The reaction in each droplet can be individually controlled by illumination with blue light through an optical fiber. We found that in pairs of BZ droplets, only the in-phase and the forcing oscillation modes are stable, however switching between these modes is not reliable. In triplets of droplets, switching between two different, stable rotational modes (clockwise and anticlockwise) can be easily implemented. Therefore, such a system is an excellent candidate for a light controlled, reliable, one bit chemical memory unit.

1 Introduction

Unconventional computing is the field of research concerned with strategies of computation that are alternatives to the standard approach, based on von Neumann architecture.[1] The interest is motivated by technological limitations in the production of integrated circuits[2] and the anticipated violation of Moore's law.[3,4] Chemical systems play a special role among the considered computing media, because of their similarity to biological information processing.[5–8]

Within chemistry-based computing there are many studies on information processing with reaction–diffusion media.[9,10] The Belousov–Zhabotinsky (BZ) reaction[11] seems to be an excellent phenomenon for such studies. It exhibits complex temporal (excitability, oscillations, chaos) and spatio-temporal (pulses, structures) behavior that can be used for information coding. A local state of BZ medium can be easily observed because usually the colors of the oxidized and reduced forms of the catalyst are distinctly different. Propagating color pulses spreading in the system correspond to a high concentration of the oxidized catalyst that follows medium excitation (*i.e.* a rapid increase in the concentration of the BZ activator).

The commonly used translation of spatio-temporal structures into information is based on the assumption that chemical excitation corresponds to the logical "TRUE" state and a non-excited medium represents the logical "FALSE" state. Information is processed in areas where excitation pulses interact. The required interactions between propagating pulses can be forced by a cleverly selected geometry of active (excitable or oscillatory) and non-excitable regions of the medium that are characterized by a strongly attractive stable state.[10,12] Therefore, the selection of geometry determines the information processing function of the computing medium. As a consequence, to change this function, one has to rearrange the medium structure, thus to re-wire the system.

A recent promising approach to BZ-based computing uses active medium encapsulated in droplets.[13–15] These are surrounded by a solution of lipids in an organic phase. The lipids organize into a monolayer on the droplet surface and provide mechanical stability. For droplets in contact, they form a stable bilayer at the interface, permeable for some of the BZ species. The coupling between droplets can have an activatory or inhibitory character depending on the organic phase and the distance. For decane and soybean lipids used in our experiments, the lipid bilayer can be penetrated by the activator of the BZ reaction ($HBrO_2$) and the activatory coupling is dominant.[16–18] As a result, excitations can pass from one droplet to another and droplets communicate.[16]

A droplet system has a few obvious advantages over an active, spatially continuous medium in the form of a membrane with an active catalyst on it.[18] First, large arrays of droplets can be automatically generated in microfluidic devices.[19–24] Second, encapsulation of the BZ reaction into droplets seems to be more flexible because it can be controlled in each droplet individually. Third, the structure of droplets, exchanging excitation pulses, resembles an active assembly of

Institute of Physical Chemistry, Polish Academy of Sciences, Kasprzaka 44/52, 01-224 Warsaw, Poland. E-mail: kgizynski@ichf.edu.pl; Fax: +48 22 343 3333; Tel: +48 22 343 3191

biological neurons. Transmission of signals in both cases is based on activation of individual, nonlinear elements. Therefore, a properly designed BZ droplet system can mimic to some extent the functionality of a human nerve system. Following this analogy, we investigate the potential of encapsulated BZ medium to realize one of the most basic function of neural networks *i.e.* information storage. It has been shown theoretically and experimentally that lipid-coated BZ droplets can be applied for information processing tasks,[16,25,26] yet the problem of constructing memory cells in such a system has not been resolved.

There have been many studies on different concepts of chemical memory.[12,27–32] Most of them were based on computer simulations with little attention to experimental proof of memory functionality. Here, we report experimental results on two and three coupled oscillating BZ droplets as potential candidates for a simple, chemical memory cell. Such a system can perform memory functions if: (i) it has (at least two) different stable oscillation modes[33–35] and (ii) it allows for switching between these modes to ensure reliable memory re-writing. Our study has been inspired by the research of Yoshikawa and his collaborators on coupled PET bottle oscillators.[33–35] In those experiments, they were able to identify a number of stable oscillatory modes that can be used as a memory device. Our experiments on BZ droplets revealed that only a fraction of coupled oscillations observed for the PET bottle case remain stable for interacting BZ droplets. We have shown that for a pair of coupled droplets, forced oscillation modes are the most stable. For triplets of droplets, clockwise and anti-clockwise rotational modes are highly stable. We demonstrate that, as in ring memory operating with a continuous excitable medium,[27] the information remembered by three droplets in the form of rotational mode direction can be stored for a long period of time. Unlike the PET bottle system, the rotational modes of three BZ droplets can be easily changed by an external factor (illumination).

This paper is organized as follows. In Section 2, we describe the experiments. Section 3, containing our results, is divided into three subsections: 3.1 – demonstration of oscillation control in separated droplets, 3.2 and 3.3 – studies on coupling oscillatory modes in two and three interacting droplets, respectively. Conclusions are presented in Section 4.

2 The experiment

For experiments, reagent grade commercially available chemicals were used without further purification. The photosensitive BZ reaction solution contained water, sulfuric acid (H_2SO_4), sodium bromate ($NaBrO_3$), malonic acid ($CH_2(COOH)_2$), potassium bromide (KBr), bathoferroin ($[Fe(batho)_3]^{2+}$) and ruthenium ($Ru(bpy)_3Cl_2$). The two latter species are catalysts for the BZ reaction. Bathoferroin tris(1,10-bathophenanthrolinedisulfonic acid) is also a redox indicator. It is red in the reduced state and pale green when oxidized. Therefore, regions containing a high concentration of the oxidized catalyst can be observed optically. The ruthenium complex (tris(bipyridine)ruthenium(II)dichloride) sensitizes the reaction to blue light ($\sim$460 nm) and allows oscillations to be inhibited in the illuminated areas.

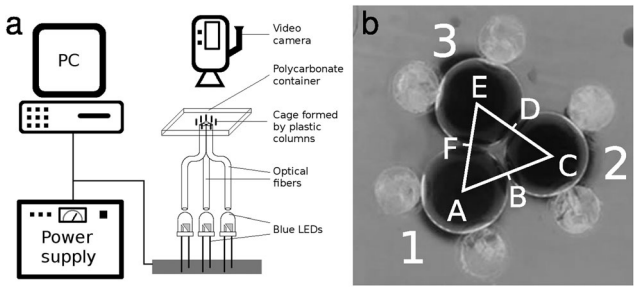

Fig. 1 (a) The experimental setup. Each droplet was separately illuminated with blue light, transmitted through optical fibers with the tips attached to the bottom of the container, centrally below the corresponding droplets. The illumination time was controlled using a PC with 1 ms time resolution. (b) The top view of 3 droplets inside a plastic columnar cage. The stabilizing columns are seen as transparent disks. A cut along the white line was performed on the sequence of frames to analyze time evolution of oscillations. Letters A, C and E mark the points at which the excitation times were measured.

Droplets containing BZ solution were prepared by pipetting small amounts (1.3 μl) of BZ reagent solution into a transparent, polycarbonate container, filled with a solution of asolectin (Sigma Aldrich #11145) in decane (0.25 g/50 ml). A number of plastic columns (0.75 mm diameter) were attached to the bottom of the container to form a cage immobilizing the droplets. The experimental system is schematically illustrated in Fig. 1.

A short time after reaching the bottom of the container, the droplets, driven by gravity, flattened on the surface forming nearly two dimensional disks. The flattening droplets, blocked by the stabilizing columns, expanded towards each other, forming a stable lipid bilayer that can be penetrated by the activator of the BZ reaction.[21,22] This chemical communication between droplets was maintained during the experiment. For the considered size of droplets (*ca.* 1.5 mm) chemical excitations were observed as centrally symmetric waves (self-excitation) or as traveling waves expanding from the contact area (activation by an excited neighboring droplet). No other, more complex forms of excitation were observed.

Chemical oscillations in the droplets were controlled by illumination with PC-controlled, high power, blue LEDs (Huey Jann Electronic, HPE8B-48K5BF, 5W, λ = 462 nm). Plastic optical fibers (1.5 mm diameter), attached to the diodes, allowed each droplet to be illuminated individually. Light emitting fiber tips were positioned centrally below the corresponding droplets. For the pairs and triplets of droplets, the intensity of the applied blue light, measured at the fiber tips using a CENTER 337 lightmeter (Center Technology Corp.), was 15 klx. All experiments were carried out at 25 °C.

Droplet activity was recorded using a digital video camera (Sony HDR-XR550VE) with a magnifying converter Raynox-505 at a resolution of 1440 × 1080 pixels and a frequency of 50 frames per second (fps). A green filter covered the camera objective to prevent damage to the CCD matrix by intensive light. Recorded movies were cut into frames and processed using ImageJ software.[36]

3 Results and discussion

3.1 Light influence on oscillations in a BZ droplet

It is well known that in the ruthenium catalyzed BZ reaction, blue light increases the concentration of bromide ions and inhibits the reaction.[37,38] The period of oscillations in the illuminated medium increases with light intensity up to a threshold value above which, no oscillations are observed.[39] The process is reversible and the medium oscillates again when illumination is switched off.

In experiments with separated droplets, we used a mixture of catalysts similar to the one reported by Toiya *et al.*[40] replacing ferroin(phen) with bathoferroin instead. The concentrations of the reagents were: 0.36 M H_2SO_4, 0.375 M $NaBrO_3$, 0.125 M $CH_2(COOH)_2$, 0.04 M KBr, 0.00125 M $[Fe(batho)_3]^{2+}$ and 0.00021 M $Ru(bpy)_3Cl_2$.

Fig. 2 shows the influence of blue light (6 klx) on the oscillations in six, unconnected droplets. The droplets were separated by a distance of 2.57 mm (see Fig. 2a), which seems large enough to consider them as independent oscillators. Droplets 1, 2, 4 and 5 were exposed to blue light at two time intervals [220 s, 405 s] and [740 s, 948 s]. The oscillations of the other droplets (3 and 6) were not perturbed. Initially, in the time interval [0 s, 220 s], all droplets oscillated with identical periods ($T \sim 35$ s).

Fig. 2b shows that the sequence of illuminations does not change the inherent period of the oscillations. When illumination is switched off, the period as a function of time is the same for both illuminated and non-illuminated droplets. It indicates that illumination does not generate reagents that remain in the medium for a long time and change its further activity. A droplet is a closed reactor and T changes slowly with time as seen in Fig. 2b. At the beginning of the experiment, the period is slightly longer than 500 s later. Next, it increases again. Such a trend is commonly observed in BZ droplet systems.[25] The initial decrease can be related to bromination of lipids and the final increase to depletion of reagents. The appearance of the first excitation after illumination seems to be unrelated to the pre-illumination phase. The first excitation was observed *ca.* 25 s after the first perturbation and *ca.* 19 s after the second one. Our results show no correlation between the pre-illumination phase and the appearance of post-illumination excitation. A more detailed comparison of time evolution for the illuminated droplet 2 and the reference droplet 3 is shown in Fig. 2c showing the intensity of green color at the droplet centers. After the first illumination, oscillations of the illuminated droplet were delayed by 5 s with respect to the non-illuminated one. The next illumination increased the delay by an additional 18 s. This result illustrates that individual optical control of chemical activity in BZ droplets can be used to generate the required phase difference between their oscillations.

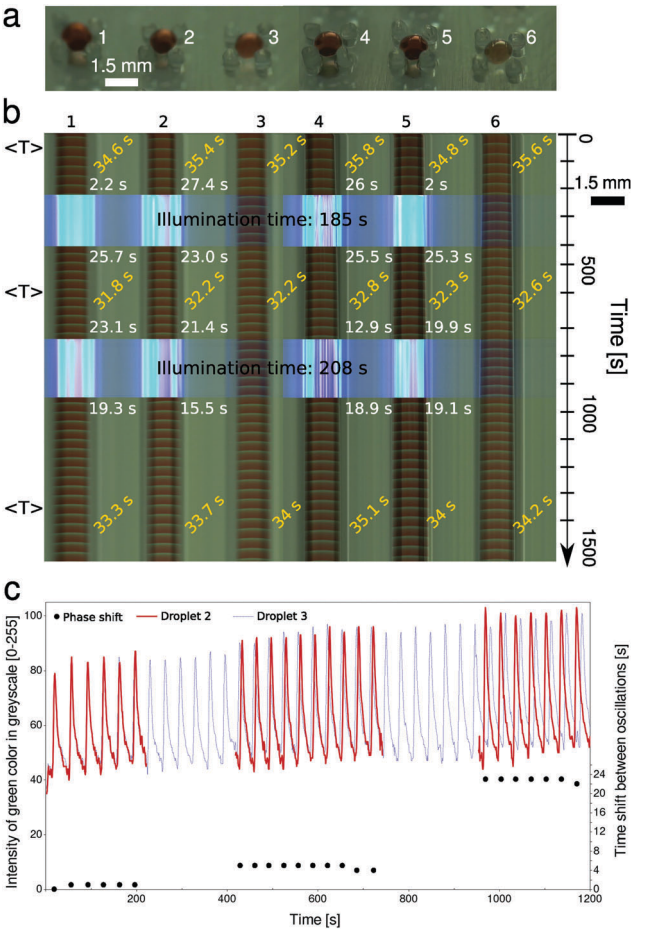

Fig. 2 Time evolution of oscillations in six uncoupled BZ droplets geometrically arranged as shown in (a). Droplets 1, 2, 4 and 5 were illuminated at two time intervals [220 s, 405 s] and [740 s, 948 s] marked as bright rectangles in the space-time plot (b); droplets 3 and 6 were not illuminated. The moments of time at which the concentration of oxidized bathoferroin in a droplet was high, can be seen in (b) as thin horizontal lines. The time between two concurrent lines defines the period of the oscillations. The averaged periods $\langle T \rangle$, (inclined numbers), are calculated for three time intervals: before, between and after illumination. The times indicated with the white color show the difference between last/first excitation and the illumination interval. (c) Intensity of green color corresponding to concentration of the oxidized catalyst, as a function of time in droplet 2 (red solid line) and droplet 3 (blue dashed line). Points below the intensity plot mark the time shift between oscillations in the droplets, measured as the time difference between the corresponding intensity maxima.

3.2 Pairs of droplets

We performed 33 experiments with pairs of coupled droplets trapped in plastic cages (see Fig. 3a). The droplets contained the following BZ solution: 0.3 M H_2SO_4, 0.375 M $NaBrO_3$, 0.125 M $CH_2(COOH)_2$, 0.04 M KBr, 0.0015 M $[Fe(batho)_3]^{2+}$ and 0.00021 M $Ru(bpy)_3Cl_2$. For the considered concentrations of reagents, the droplets spontaneously started to oscillate just after pipetting with a period $T = 60$ s. Their initial phases were random.

One of experiments in which oscillation modes are switched optically is illustrated in Fig. 3. As shown in the space-time plot (Fig. 3b), initially chemical excitations were spreading out of the center of droplet 1 (marked schematically with a solid, semi-circular line) towards the boundaries and after passing through the lipid bilayer they propagated into droplet 2 (marked with a dashed line). The initial mode was stable. This type of droplet

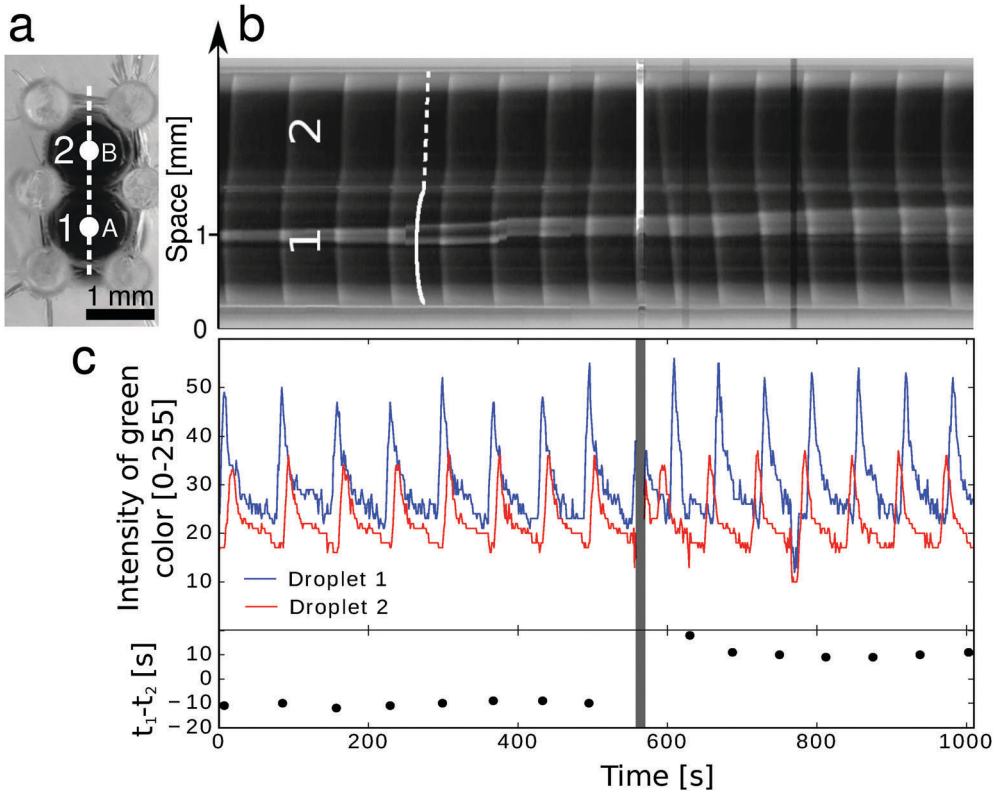

Fig. 3 (a) Top-view of a pair of coupled BZ droplets trapped in a plastic cage. (b) The space-time plot along the white line shown in (a). The white rectangle marks illumination applied to droplet 2 (SDI 10 s). (c) The intensity of green color (top) and the time shift between excitations (bottom) observed at points A and B. The grey vertical bar marks the time interval at which illumination was applied. Notice that after illumination the oscillation mode changed from (3a) into (3b) (*cf.* Fig. 4).

interaction is defined as a forcing mode since excitations of droplet 1 forced excitations in droplet 2. After illumination, the activation sequence was reverted, *i.e.* excitations were transferred from droplet 2 to 1. The induced mode was also stable and the time difference between the excitations at the droplet centers was the same (with opposite sign) as before illumination.

3.2.1 Classification of oscillations in a pair of droplets. The classification of different oscillating modes for a pair of droplets with similar frequencies is illustrated in Fig. 4. In the cases where the initial phases are nearly identical (both droplets excited at the same time), in-phase oscillations are expected. If the phase difference is small, the droplet that is excited first becomes a pacemaker, forcing oscillations in the second one. Finally, for a large initial phase difference, anti-phase oscillations may appear as described later.

In order to quantify different modes of oscillations in a pair of droplets, we introduced the phase difference $\Delta\varphi$ defined as $\Delta\varphi = 2\pi\frac{t_2 - t_1}{\langle T\rangle}$, where t_i is the moment of excitation in the droplet (i) and $\langle T\rangle$ is the averaged period of oscillations at the corresponding stage of the experiment. The times of excitation in the droplets were measured at their centers (marked in Fig. 3a with letters A and B for droplets 1 and 2, respectively). The phase difference for the in-phase mode is $|\Delta\varphi| < 0.1\pi$. For the forced oscillations, there is a small difference between the excitation times due to propagation of excitation between the droplet centers and $0.1\pi \leq |\Delta\varphi| \leq 0.5\pi$. The upper and lower estimation of $\Delta\varphi$ comes from experiments in which forcing was observed on a space-time plot. The values of $\Delta\varphi \in (0.5\pi,\pi\rangle$ are characteristic for anti-phase oscillations.

In an oscillation cycle, we can distinguish the excited phase **E** where the concentration of the activator is high. This phase is followed by the refractory phase **R** with a high concentration of the inhibitor. A droplet is insensitive to perturbations coming from its neighbors during the refractory phase. The concentration of inhibitor drops in the responsive phase **Q**. In this phase, a droplet can get excited by an excited neighbor. If there is no external perturbation, self-excitation occurs and the cycle repeats. Then the period sums up to $T = |E| + |Q| + |R|$, where the symbol $||$ denotes the length of the corresponding phase. Anti-phase oscillations can appear when one droplet is in the refractory state at the time the other is excited. Furthermore, as shown in Fig. 4b, stationary anti-phase oscillations are possible only when the following conditions hold: $|t_2 - t_1| < |R|$ and $T - |R| = |Q| + |E| < |t_2 - t_1|$. Therefore, if the length of the refractory phase is known, then any phase difference that satisfies the condition $2\pi(1 - r) < \Delta\varphi < 2\pi r$, where $r = \frac{|R|}{\langle T\rangle}$, can be associated with the anti-phase oscillations. Note that such phase differences are located around the value of π. If the refractory phase is short ($|R| < T/2$) then there are no stationary anti-phase oscillations in a pair of coupled droplets. The range

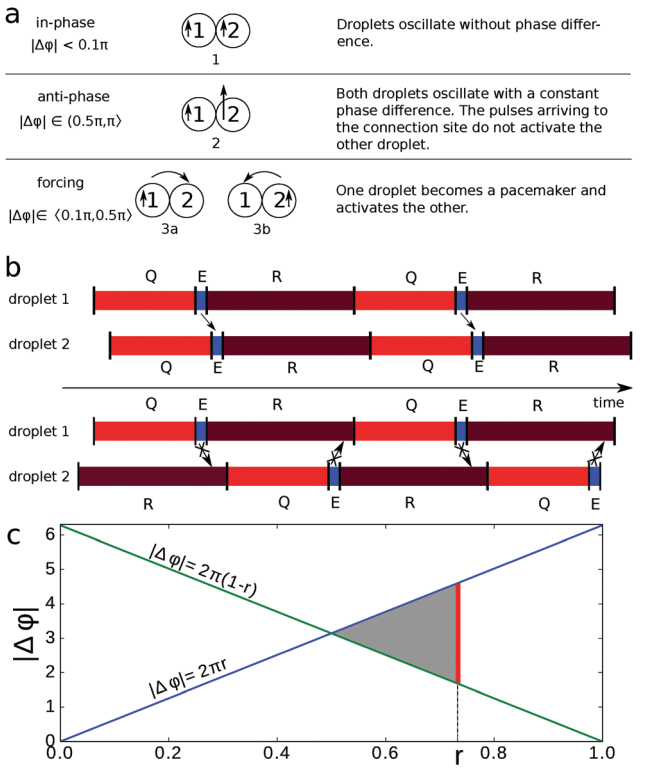

Fig. 4 (a) Classification of modes for a pair of coupled BZ droplets. Vertical arrows correspond to pulses spreading homogeneously from the center of the droplets outwards. The phase difference between droplets is marked with the length of the shafts. Propagation of a chemical excitation between droplets (activation process) is schematically illustrated with arrows pointing from one droplet to another. (b) Schematic illustration of coupling between droplets in forcing and anti-phase modes. (c) The vertical line shows the range of phase shifts corresponding to the anti-phase modes for a selected value of r.

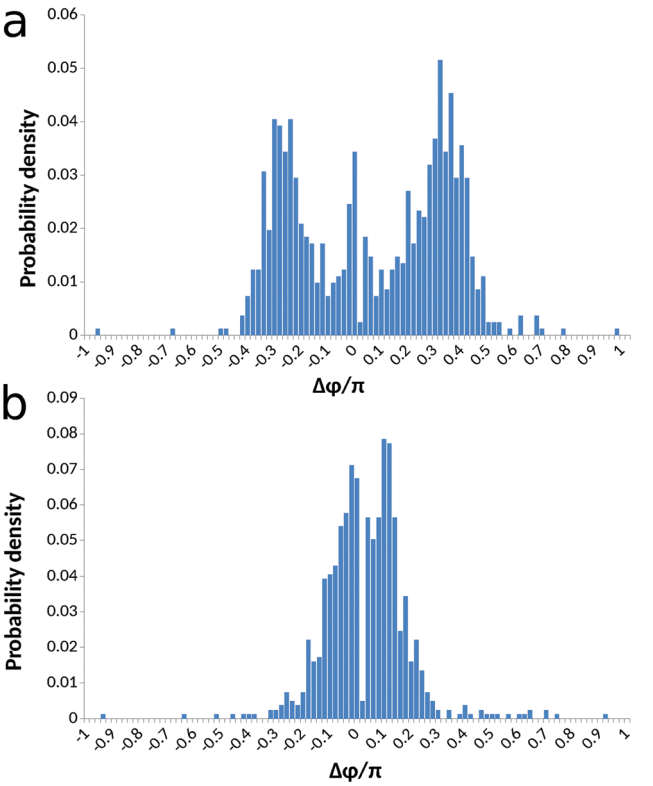

Fig. 5 The probability distribution of phase differences from all experiments. $\Delta\varphi$ calculated with t_1 and t_2 describing times of excitations (a) at the droplet centers, and (b) on both sites of the lipid bilayer separating the droplets.

of $\Delta\varphi$ corresponding to the anti-phase mode is determined by r, describing the ability of the coupled droplets to exchange excitations. However, it seems difficult to estimate this value even if the geometry of a bilayer separating droplets is known. Propagation of chemical activation between droplets is a complex process[43] and it can be influenced by many factors that are hard to control. For example the local charges on a membrane can change the diffusion of particles (like the activator) and modify the activation times.[44]

3.2.2 Optical switching between oscillation modes. The probability distribution of phase differences observed in our experiments with pairs of droplets are shown in Fig. 5. There are three pronounced maxima corresponding to the (1), (3a) and (3b) modes. Due to the dominant activatory coupling, the probability of mode (2) is very small, but still non-negligible. The comparison of Fig. 5a and b indicates that large values of $|\Delta\varphi|$ are not related to long times of excitation propagation through the lipid bilayer, but correspond to anti-phase oscillations. The most frequently observed modes are potential candidates for the memory states. In the following, we concentrate on optical switching between them.

Two illumination scenarios were applied to switch between different oscillation modes. In the first one (both droplet illumination, BDI), droplets were allowed to oscillate in dark conditions for a few periods. Next, both of them were

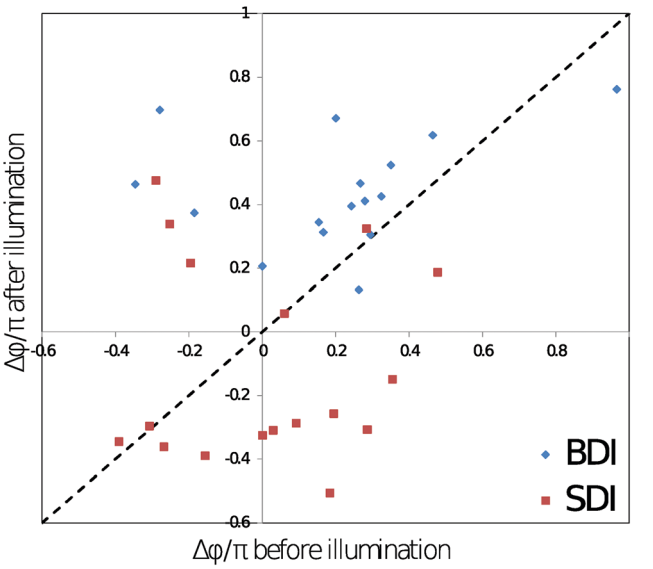

Fig. 6 Phase difference ($\Delta\varphi$) in pairs of coupled droplets in the first cycle after illumination as a function of $\Delta\varphi$ in the last excitation before illumination. $\Delta\varphi$ after illumination is calculated as the time difference between excitations seen after turning off all diodes. The cases in which $\Delta\varphi$ was not changed by illumination are located close to the dashed line representing the function $y = x$.

illuminated with an identical light intensity (6 klx) for a time interval equal to the inherent oscillation period (60 s). Then illumination of one droplet was switched off and illumination of the other one continued with the same light intensity. The considered lengths of additional illumination were 4 s, 28 s, 30 s, 32 s, 45 s and 56 s. By selecting additional exposure times close to $T/2$, we expected to stabilize anti-phase oscillations. In the other scenario (single droplet illumination, SDI) only one of the droplets was illuminated, whereas the other one evolved in the dark. We considered SDI times of: 5 s, 10 s, 15 s, 20 s and 30 s.

At the initial stage of the experiment, oscillations in coupled droplets evolved into a stable mode. As seen from the arguments of the results presented in Fig. 6, the anti-phase and the in-phase modes appeared spontaneously in only 1 and 5 out of 33 cases respectively. For the majority of pairs, the initial $\Delta\varphi$ was within the range $[-0.5\pi, -0.1\pi] \cup [0.1\pi, 0.5\pi]$ indicating that the forcing mode was the most stable. This conclusion is supported by results for $\Delta\varphi$ after illumination shown in the same figure. There was only 1 case in which in-phase oscillations were observed just after illumination and a few cases in which a large phase difference was generated. In the remaining experiments, forcing mode oscillations appeared immediately after illumination. The points located close to the dashed line in Fig. 6 represent the cases in which the mode remains unchanged by the applied illumination (*e.g.* for BDI 60 s + 4 s and SDI 5 s). These points make half of all cases, which suggests that switching the oscillation mode in a pair of droplets using either of these two strategies is likely to fail.

Fig. 6 shows $\Delta\varphi$ for the first oscillation observed after illumination terminates. However, in many cases, the mode obtained just after illumination was not stable and evolved into another one. A few examples are shown in Fig. 7. In each experiment, we observed the time evolution of droplets for a few cycles preceding and following the illumination (*cf.* space-time plots in Fig. 3b and 7e). The results of an experiment are presented as the dependence of the phase difference corresponding to the pair of next excitations ($\Delta\varphi(n+1)$) as the function of the previous phase difference ($\Delta\varphi(n)$). The straight arrows connecting the points determine the trajectory of the oscillation

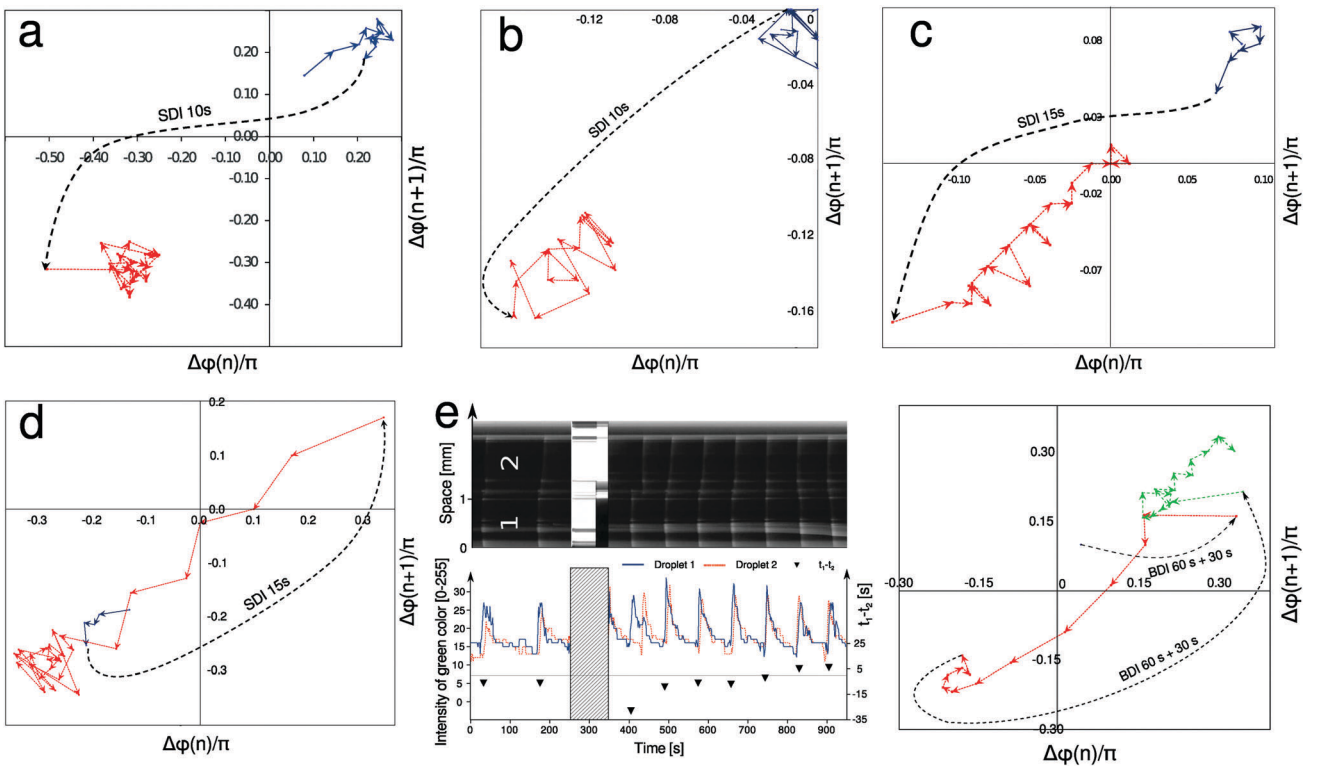

Fig. 7 Time evolution of oscillation modes in selected experiments with two droplets. The points and trajectories marked with colors blue, red and green correspond to the initial, spontaneous evolution of oscillations and the oscillation modes after the first and the second optical perturbation respectively. Green color is used only for cases when the droplets were illuminated two times. The dashed, curved arrows join the last mode before illumination (shaft) and the first mode after (head). (a) Successful, stable mode reversing from (3a) to (3b) after 10 s SDI applied at t = 975 s. The analysis of the oscillations and the space time plot (of part of the experiment) are shown in Fig. 3b and c. (b) Successful switching from mode (1) to (3b) after 10 s SDI applied at t = 1038 s. (c) A mode reversing from (3a) to (3b). 15 s SDI was triggered at t = 852 s. The obtained (3b) is unstable and the system evolves towards mode (1). (d) Unstable mode reversing from (3a) to (3b). 15 s SDI applied at t = 764 s. (e) Complex mode evolution after two BDI 60 s + 30 s perturbations. The first illumination was applied at t = 246 s and it generated an unstable (3a) mode that spontaneously evolved towards a stable (3b) mode. The next BDI 60 s + 30 s, applied at t = 1432 s, generated a stable (3a) mode. The space-time plot and the green color intensity as a function of time for the initial stage of the experiment are shown on the left. The applied illumination is visible as bright rectangles on the space-time plots and hatched areas on the time series.

mode in the phase space $\Delta\varphi(n+1) \times \Delta\varphi(n)$ and indicate the direction of time. A stable mode in this representation can be seen as a small area located close to the $\Delta\varphi(n+1) \simeq \Delta\varphi(n)$ line with a large density of points.

Fig. 7a illustrates a successful transition between two forcing modes: (3a) and (3b), resulting from 10 s illumination of droplet 2 (SDI 10 s). The space-time plot and the time evolution at point A and B are shown in Fig. 3a and b. Fig. 7a confirms that both initial and induced oscillation modes were stable. The trajectory is confined into small domains of phase space corresponding to modes (3a) and (3b) respectively. Another example of a successful transition between different modes is shown in Fig. 7b where a stable in-phase mode (1) was changed into the stable mode (3b) after 10 s of SDI. Fig. 7c illustrates the case in which mode (3a) was switched into the mode (3b) by 15 s of SDI. In this case, the forced (3b) mode is not stable and the system evolved spontaneously towards the stable in-phase mode (1). Such a result is not surprising because the initial (3a) mode was not stable and evolved towards the mode (1). Another case for which the oscillation stability was not changed by illumination is given in Fig. 7d. The system was switched from the (3b) mode to (3a) mode by 15 s of SDI, but spontaneously returned to the initial mode. Fig. 7e shows a case of double illumination using the BDI (60 s + 30 s) scenario twice. The initial state was transformed into an unstable (3a) mode after the first illumination. The (3a) mode spontaneously evolved into the stable (3b) mode. The second BDI illumination switched the mode back to (3a) and the system remained stable in it. Thus, we succeeded in making mode switching, reversed to the one illustrated in Fig. 7a.

Our experiments have shown that the forcing modes are the most common type of oscillations for a pair of coupled droplets. Stability analysis of the mode evolution revealed that for most of the experiments, the light initiated mode was sustained only for a short time and then the system converged to the most stable forcing mode. We tested different illumination strategies, but none of them allowed for reliable stabilization of oscillations in a different mode. This conclusion is supported by results located in the diagonal cells of Table 1 summarizing stable mode modifications from all experiments. The high stability of a single forcing mode can be attributed to various inherent periods of droplets. Although the droplets contained the same BZ solution, different frequencies can appear due to differences in hard-to-control parameters of droplets like radius,[22,42] shape or contact area with the column cage *etc.* After some time, a pair of droplets oscillates in a forcing mode with the higher droplet frequencies which is in agreement with previous reports on coupled BZ droplets.[21,41] The fact that in so many cases, a two droplet system returns spontaneously to its stable oscillation mode makes it useless as chemical memory.

Table 1 Number of stable modes observed after illumination with respect to the stable pre-illumination modes

The stable mode after illumination	The stable mode before illumination			
	1	2	3a	3b
1			3 (3 SDI)	
2			1 (1 BDI)	
3a	1 (1 BDI)	1 (1 BDI)	13 (9 BDI, 4 SDI)	
3b	3 (1 BDI, 2 SDI)	1 (1 BDI)	1 (1 SDI)	9 (2 BDI, 7 SDI)

3.3 Triplets of droplets

In this section, we describe oscillation modes in the system composed of three coupled droplets arranged in a regular triangle geometry (see Fig. 1a). We carried out 22 experiments and in all cases, we observed coupling between droplets. In 10 experiments, we used the same concentrations of reactants as in the previous section. More than half of the experiments (12) were performed with modified concentrations of sulfuric acid, bathoferroin and ruthenium, in order to obtain a medium with shorter oscillation periods ($T < 30$ s, see caption of Fig. 11). After preparation of the droplets, we used illumination to initialize a specific mode and next, we observed the time evolution of the droplets. The applied illumination strategy

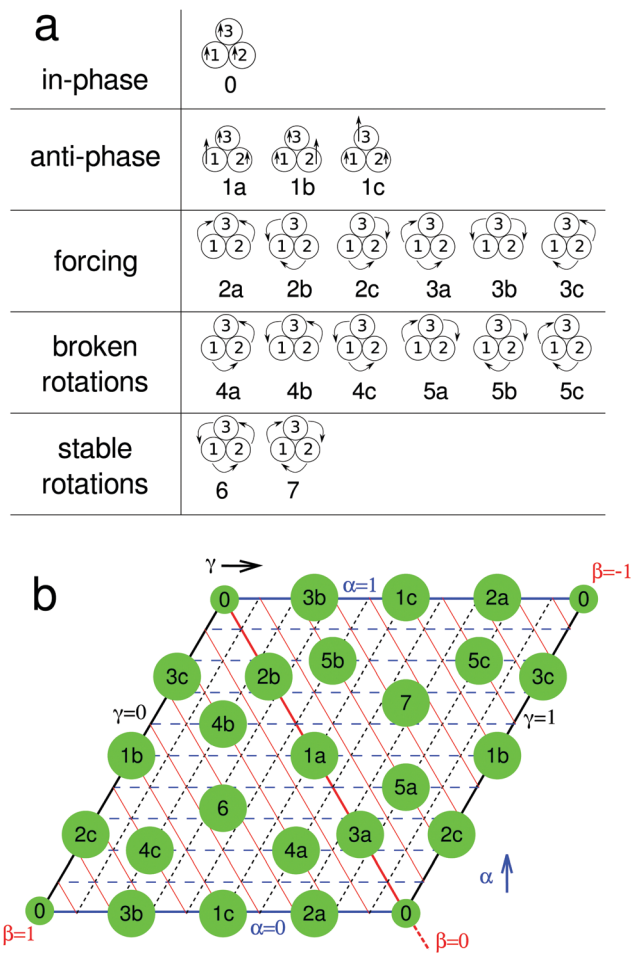

Fig. 8 (a) The modes of coupled oscillations expected for a triplet of coupled BZ droplets. The meaning of the arrows is the same as in Fig. 4a. (b) The geometrical representation of the stable modes in the rhomboidal plot with coordinates α, β and γ.

was similar to the BDI method described previously, yet an additional exposure, applied to the third droplet was added.

3.3.1 Classification of oscillations in a triplet of droplets. If all droplets are identical, then assuming symmetry of the system, the coupled oscillation modes listed in Fig. 8a are expected. Similarly to the two droplet case, the in-phase mode corresponds to a situation where all droplets get excited at the same time, whereas in the anti-phase mode, the excitations in one droplet are shifted in time with respect to the others by $T/2$.

There are two classes of oscillations that belong to the forcing modes. In modes 2a, 2b and 2c the coupled in-phase excitations of two droplets activate the third one. The other class (modes 3a, 3b and 3c) corresponds to the case where excitations in one of the droplets force synchronized excitations of the other two. For both types of forcing modes, the time difference between excitations at the droplet centers is much smaller than $T/2$ and it is related to the time in which an excitation pulse propagates between droplets.

In the forcing modes described above, oscillations of two droplets were in-phase. We also observe another type of forcing mode, in which a cascade of excitations is observed: one droplet excites another and the excited droplet forces excitations in the third one. If the refractory time of the medium is longer than the time in which an excitation passes from the first droplet, through the second, to the third one, the propagation of excitation terminates at the third droplet, because the level of inhibitor in the first droplet is still high, so it cannot re-excite. As a result, we observe a single rotation of excitation pulse through all droplets, followed by a long time when the system shows no activity. We call such mode a broken rotation. The broken rotation can circulate anticlockwise (4a, 4b, 4c) or clockwise (5a, 5b, 5c). If the refractory period is shorter than the time within which an excitation travels between droplets, then the first droplet is in the responsive state when excitation from the third droplet arrives. As a consequence, a pulse of excitation smoothly rotates between droplets. Such a pulse can be seen as an analogue of a spiral wave in a spatially continuous medium. Importantly, spiral waves are characterized by higher frequency than the inherent period of the medium and thus are highly stable.[45] Here we distinguish two rotational modes: anticlockwise (6) and clockwise (7).

The modes described above can be easily visualized. Let us assume that pulses of excitation (maxima of oxidized catalyst concentration) appear at the centers of droplets 1, 2 and 3 at times t_1, t_2, t_3 and t_1' respectively, where t_1' is the time of consecutive excitation in droplet 1. Then, we introduce variables α, β and γ defined by the following equations:

$$\alpha = \frac{t_2 - t_1}{t_1' - t_1}, \quad 0 \le \alpha \le 1 \tag{1a}$$

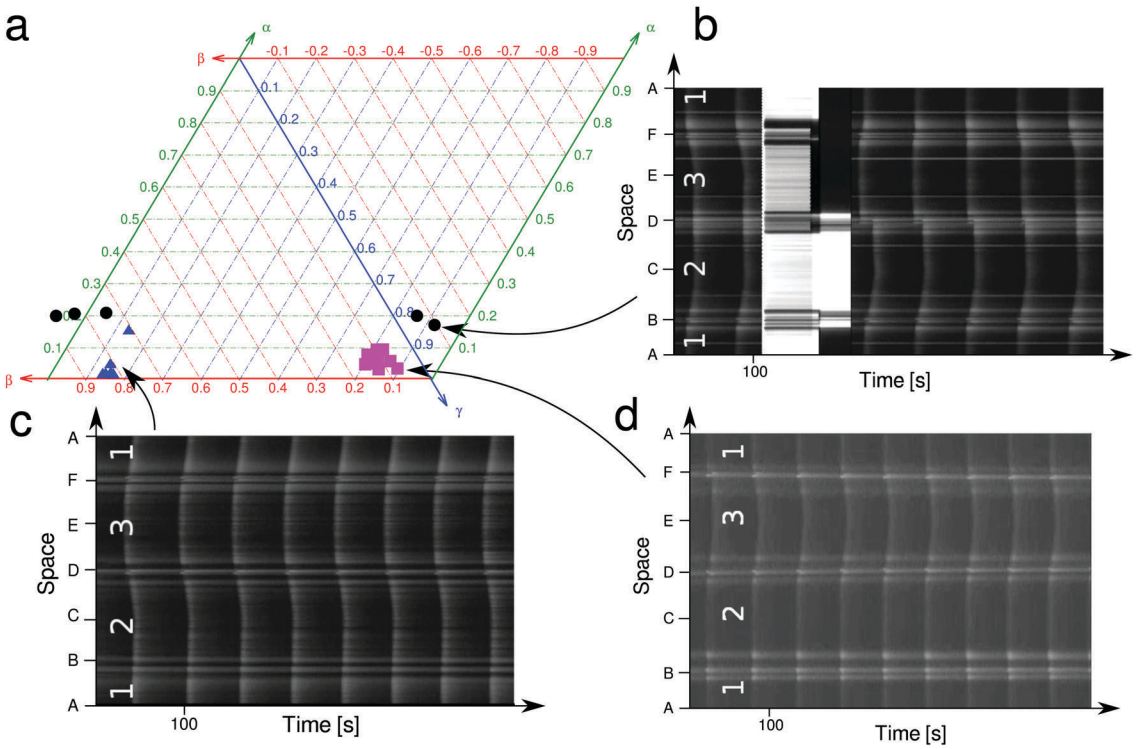

Fig. 9 Common oscillation modes observed after placing three droplets in the cage (*cf.* Fig. 1). (a) Geometrical representation on the rhomboidal plot of the modes shown in (b–d). Circular, triangular and square points correspond to the modes presented in (b), (c) and (d) respectively. A high density of points in one area indicates mode stabilization. Space-time plots from (b–d) were generated by cutting frames from the experimental movies along the bright lines visible in Fig. 1a. The points A, C and E mark the geometrical centers of droplets 1, 2 and 3 respectively, whereas the points B, D and F indicate contacts between the droplets. (b) Instability of anticlockwise broken rotations. Before illumination the droplets oscillate in the (3a) mode. The induced (4c) mode visible for the first pulses after switching off the light changed back to (3a) for the next oscillation cycles. The light exposure times for droplets 1, 2 and 3 were 70 s, 110 s and 60 s respectively. (c) The (3b) forcing mode. (d) The forcing mode (2a) with two pacemakers oscillating in phase (droplets 1 and 2).

$$\beta = \frac{t_3 - t_2}{t_1' - t_1}, \quad -1 \le \beta \le 1 \tag{1b}$$

$$\gamma = \frac{t_1' - t_3}{t_1' - t_1}, \quad 0 \le \gamma \le 1 \tag{1c}$$

and $\alpha + \beta + \gamma = 1$. Every oscillation mode in a system of three coupled droplets can be represented by a point on a rhomboidal plot composed of two regular triangles with a height equal to 1. A triplet of numbers (α, γ, $|\beta|$) describes the distances of the point from the bottom and left rhomboid sides and from the diagonal respectively. It turns out that the triangle representing (α, $|\beta|$, γ) has one side common with the triangle representing (α, $-|\beta|$, γ). The geometrical representation of the modes is illustrated in Fig. 8b.

3.3.2 Optical switching between rotating oscillation modes. Having in mind the instability of forcing modes observed for pairs of droplets related to system evolution towards the forcing mode characterized by the shortest period and high stability of spirals in a continues medium, we focused here on the rotational modes. In order to generate a rotational mode, a different illumination time was applied to each droplet. In such cases, the droplet with the shortest exposure is excited first, next the one with medium illumination time and finally excitations of the droplet with the longest exposure appear. Correctly selected illumination parameters should assure that the excitation from the initial droplet can activate the second droplet only, whereas the third one would be still in a refractory state and remain unaffected. The period of the rotational modes depends on the length of the path covered by the rotating excitation and on the excitation velocity. Thus, designing chemical memory we should match the droplet sizes with the reagent concentrations in the BZ medium.

For the solution of BZ-reagents yielding oscillations with a 60 s inherent period, only in one of the experiments a stable rotational mode was observed. Usually the illumination scenario led to broken rotations. There was no re-excitation of the droplet from which excitation started because it was still in the refractory state. As a result, the time between successive excitations of droplets is similar to the inherent period of the medium. Such a broken rotation mode can be easily destroyed though, if the differences in the inherent frequencies of the droplets are significant. As in the previous case, the droplet(s) with shorter period become(s) a pacemaker and force(s) oscillations in the others. Examples of the most commonly observed modes for large inherent periods are shown on a rhomboidal plot in Fig. 9a along with the corresponding space-time plots (Fig. 9b–d). The fact that forcing modes are dominant when the oscillation period is longer than the time in which excitation passes through all droplets can be seen on the probability distribution of a mode corresponding to given values of α, β and γ shown in Fig. 10a. Three pronounced maxima correspond to modes (3a), (3b) and (3c).

The crucial factor determining successful initialization of the stable rotational mode is the state of the first droplet at the end of a cycle. The droplet must be in the responsive state to be activated when the next cycle begins. To fulfill this condition, both the size of the droplets and the concentrations of the BZ reagents have to be properly selected. In the first option, the distance for the chemical wave to travel can be increased or decreased leaving more or less time for the first droplet to recover. Here we used the other approach and simply adjusted the concentrations of sulfuric acid, bathoferroin and ruthenium to reduce the inherent period to (i) T = 28 s, and (ii) T = 24 s (for concentrations, see the captions of Fig. 11a and c). For such a high-frequency oscillating medium the probability of rotational modes is increased as compared with T = 60 s as shown in Fig. 10b, because for shorter refractory time, the contact through the lipid bilayer established in typical experimental conditions is sufficient to transmit the chemical excitation.

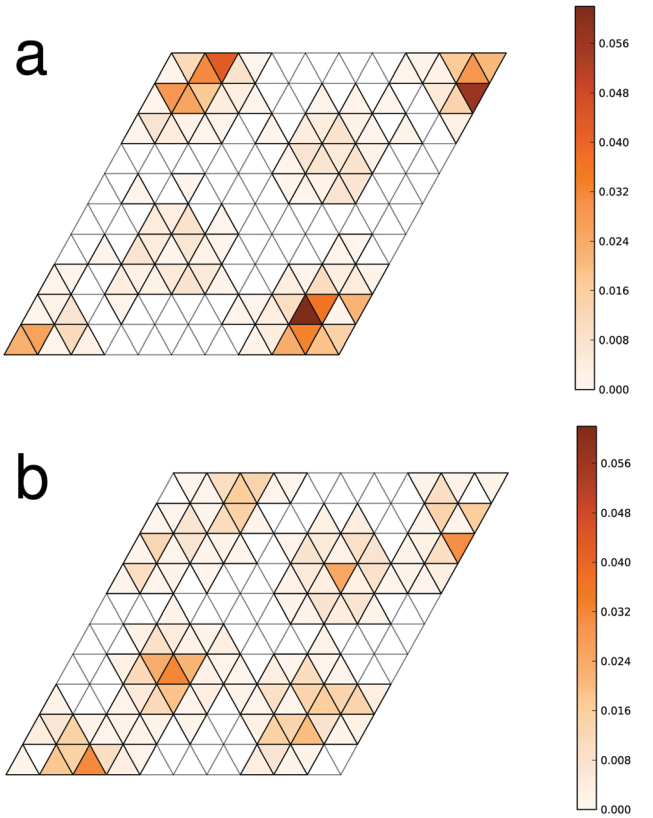

Fig. 10 Probability distribution of phase differences for triplets of coupled droplets oscillating with period (a) T = 60 s and (b) $T \le$ 30 s.

A transformation of spontaneously created forcing mode (2c) into the rotational, anticlockwise mode (6) is presented in Fig. 11a. We observed mode (6) for 145 s and then reverted the light sequence to change the direction of the rotations. After illumination, the stable, clockwise mode appeared and the system ran in this configuration for 238 s until the next mode reversing procedure. To force the anti-clockwise oscillations again, three attempts were made with different illumination conditions before we observed the required change. In both unsuccessful attempts to change the rotation direction, the same forcing mode (3c) was observed. In the third attempt, the anticlockwise mode (6) was initialized and remained stable

for 1142 s, until the end of the experiment. A good stability of rotational modes (6) and (7) compared to the oscillatory modes of the two droplet system is ensured by a high frequency of droplet excitations. For example, in the case illustrated in Fig. 11a the inherent period of the oscillations is 28 s, whereas in a rotational mode each droplet is excited every *ca.* 19 s. It is known[21] that the source of excitations, characterized by the highest frequency, becomes a stable pacemaker of an excitable medium. In the case of 3 droplets, the high frequency oscillations do not transform spontaneously into a lower frequency mode.

The precise selection of illumination time is important for reliable switching between rotational modes. Fig. 11c and d illustrate the time evolution of the droplets with the following concentrations of reagents: 0.405 M H_2SO_4, 0.375 M $NaBrO_3$, 0.125 M $CH_2(COOH)_2$, 0.04 M KBr, 0.0015 M $[Fe(batho)_3]^{2+}$ and 0.00017 M $Ru(bpy)_3Cl_2$. For such concentrations, the inherent period is 24 s. At the beginning, the clockwise rotational mode (7) spontaneously appeared. The first attempt to change it into an anticlockwise rotation with illumination times (40 s, 15 s, 26 s) applied at t = 426 s was not successful and the forcing mode (3c) appeared because the droplets 1 and 3 were in the responsive

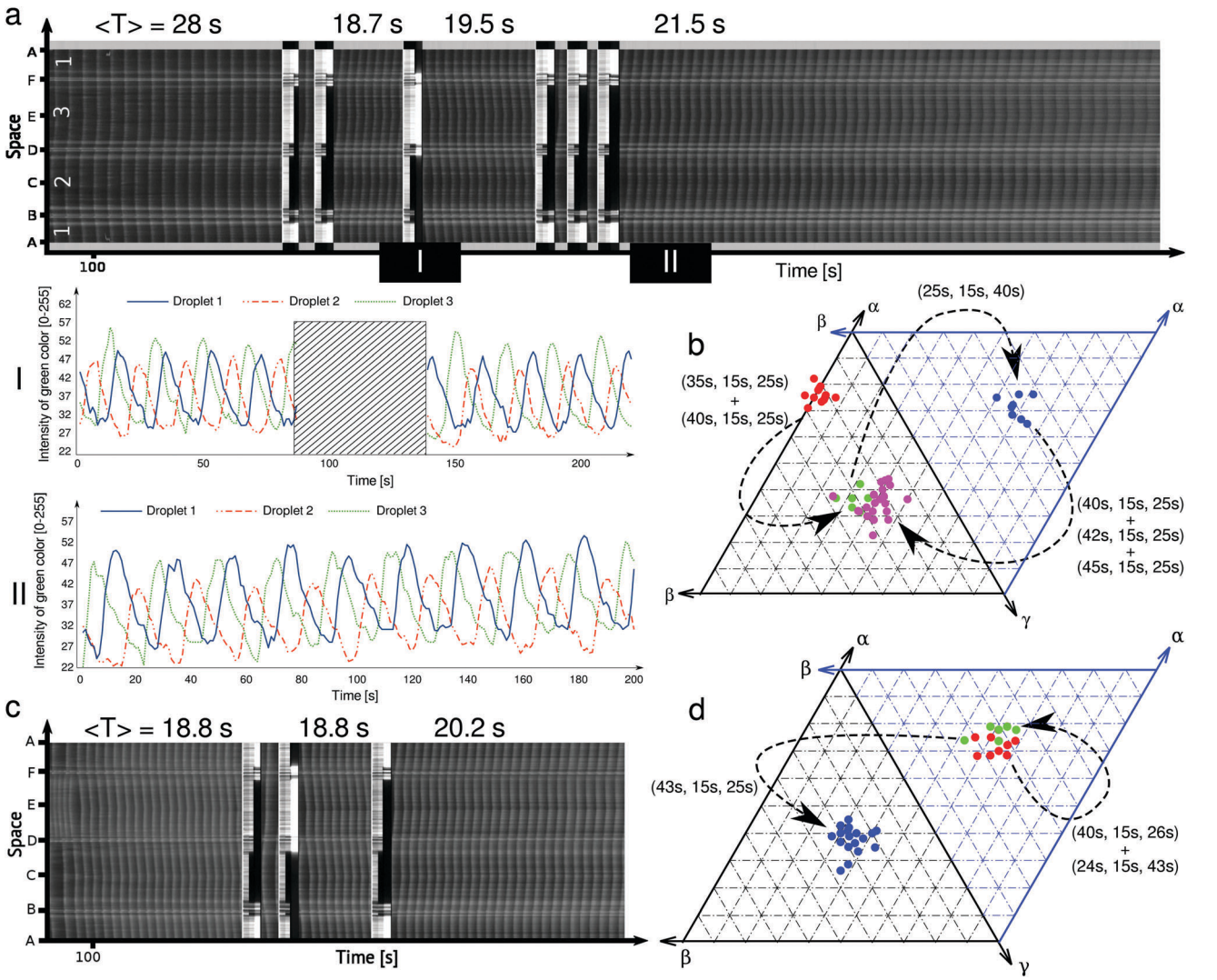

Fig. 11 Space-time plots and rhomboidal stability plots from experiments with increased frequency of oscillations. The concentrations of sodium bromate, malonic acid and potassium bromide in both cases are 0.375 M, 0.125 M and 0.04 M respectively. (a) Self-excitation period, T = 28 s obtained using 0.36 M $[H_2SO_4]$, 0.00125 M $[Fe(batho)_3]^{2+}$ and 0.00021 M $Ru(bpy)_3Cl_2$. The six following illuminations were applied to droplet 1, 2 and 3: (35 s, 15 s, 25 s) initiated at 494 s, (40 s, 15 s, 25 s) at 564 s, (25 s, 15 s, 40 s) at 750 s, (40 s, 15 s, 25 s) at 1031 s, (42 s, 15 s, 25 s) at 1098 s and (45 s, 15 s, 25 s) at 1161 s. The averaged periods $\langle T \rangle$ from the corresponding stages of the experiment are given above the plot. Time difference between excitations in droplets is illustrated for two parts of the experiment: (I) optical switching between modes (6) and (7) and (II) sustained, stable mode (6). The hatched area corresponds to the light exposure time. (b) Stability analysis of oscillation modes presented in (a). Dashed arrows correspond to light perturbations. Red, green, blue and magenta points correspond to the initial mode (3c), mode (6) induced by the first two illuminations, mode (7) after the third illumination and the final mode (6) respectively. (c) Space-time plot of the experiment with T = 24 s obtained for 0.405 M $[H_2SO_4]$, 0.0015 M $[Fe(batho)_3]^{2+}$ and 0.00017 M $Ru(bpy)_3Cl_2$. Illumination was triggered at 426 s (40 s, 15 s, 26 s), 504 s (24 s, 15 s, 43 s) and 708 s (43 s, 15 s, 25 s). (d) Stability analysis of the modes observed in (c). Spontaneous (7), first, optically induced (7) and the final (6) modes are marked with red, green and blue points.

state when illumination terminated. This mode was transformed back to the original rotations by illumination (24 s, 15 s, 43 s) triggered at t = 503 s. A small modification of the illumination times (43 s, 15 s, 25 s) compared to the first perturbation, which increased the time interval when droplet 1 was refractory, allowed us to switch the rotational mode into the required anti-clockwise mode. Note that in this case, the period of rotating oscillations is also shorter (*ca.* 19 s) compared to the inherent one, yet it is almost the same as the period in the rotational mode from the experiment shown in Fig. 11a. The fact that in both cases the modified periods are the same, confirms that if the rotational mode can be triggered, then its stable period is shorter than the inherent one and determined mainly by the size of the droplets.

Assuming that the modified period of the oscillations is determined mainly by the geometry of the system one can expect that the initialization of stable rotations is possible only if the period of self oscillations for the given concentrations is similar to the time necessary for the activation wave to travel through the structure of all three droplets sequentially. Only one experiment with successful initiation of mode (6) using the medium with a long period (60 s) was observed. After decreasing the inherent period of oscillations, we were able not only to induce a stable rotational mode but also to revert the direction of rotation twice in the same experiment as presented in Fig. 11a and b. Furthermore, for the experiments with the period decreased to 24 s, we observed the spontaneous initialization of the rotational mode that was successfully reverted using optical control as presented in Fig. 11c and d.

4 Conclusions

In this paper, we presented results of experiments on a type of chemical memory, based on oscillating BZ-droplets. In the system studied, information is coded in modes of coupled oscillations. We considered two and three droplets with the ruthenium catalyzed BZ reaction. This variant of the BZ-reaction is inhibited by illumination and we used blue light to switch between different oscillation modes.

In the case of 2 coupled droplets, we observed 3 oscillation modes with potential applications for information coding: the synchronized in-phase oscillations of both droplets and the forcing modes in which excitations of one droplet activate the other one. All these modes can be stable, but usually one of the forcing modes dominates the system over a long time scale. We believe that this is related to the fact that oscillation periods for all modes are roughly the same as the inherent period of the BZ-medium. Some differences in the period can be associated with different droplet volumes, contacts with the substrate and other factors. It is known that in an oscillatory medium, the source of the highest frequency oscillations becomes a pacemaker that dominates the time evolution. In experiments with 2 droplets we observed many cases in which an oscillating mode obtained after illumination was unstable and the system evolved towards a pre-illumination oscillating mode. Thus the optical switching between modes is not reliable. We think that oscillations in the 2-droplet system are not applicable as switchable chemical memory.

In the case of 3 coupled droplets we observed 8 stable oscillation modes, but for information storage the most interesting are clockwise and anti-clockwise rotational modes. They are characterized by a period of oscillations that is much shorter than the inherent period of the medium. Therefore, there are no spontaneous transitions to the rotational modes from a medium evolving according to another mode. In contrast, for pairs of coupled droplets, all modes are oscillating with the frequency similar to the inherent frequency of the medium and frequency does not enhance the mode stabilization needed for memory applications.

The transitions to modes (6) and (7) can be forced by a cleverly selected sequence of illumination times. It can be expected that the optical control should include initial illumination of all droplets in order to make the oscillation phase uniform, followed by individual illuminations of droplets that differ by 1/3 of the anticipated excitation rotation time. However in our system the reflection of light by an illuminated droplet affected the evolution of non-illuminated ones. Thus, the illumination sequence was adjusted to take this effect into account. We think that the diameter of the optical fiber, similar to the droplet size, was too large in our experiment and that the light should be concentrated in the droplet center.

We have also shown that one can use illumination for on-demand switching between the forcing modes, clockwise and anti-clockwise rotations. Therefore, a 3-droplet system with information coded in these states is a good candidate for chemical memory. The results in Fig. 11 show that such memory preserves its state for many oscillation cycles.

Direct downsizing of the memory based on 3 droplets seems difficult. For sub-milimeter droplets, an increase of the oscillation period (and of the refractory time) at small diameters is observed.[22] This effect is related to the escape of BZ activator into the organic phase being pronounced for larger surface to volume ratios. It acts against the decrease of the rotational mode period required for small droplet radii. We think that the presented construction of 3-droplet memory can be downsized ten times using BZ medium with a few second period. Further downscaling can be achieved with lipids that form monolayers unpenetrable for activator molecules, provided that the diffusion of the activator through bilayers, enabling droplet communication, is possible.

The experimental results (*cf.* Fig. 11a and c) suggest that we can extend the number of memory states by adding any other mode (*e.g.* a forcing mode) to modes (6), and (7). This makes 3-state memory in which information is coded in short-period, clockwise and anti-clockwise rotations and additionally in another mode with a longer oscillation period. In such an approach we assume that any of the long-period modes represent the same memory state. The periods of the modes listed in Fig. 8a except for (6) and (7) are the same as the period of the BZ-medium. Therefore, 3-state memory should be reliable, regardless of whether the additional mode is stable or not. If it is not stable then it can transform into another mode with

a similar period of oscillations, but such operation does not change the memory state. Mode stability analysis indicates that extension of 3-droplet-based memory to a larger number of logical states is impossible.

In this paper, we have intentionally not compared experimental results with simulations. There are many models that can be used to simulate oscillations in BZ-droplets.[14,15,46,47] However, the mechanism of transport in a lipid bilayer has not been described quantitatively yet. One can set parameters describing this transport and obtain qualitative agreement between simulations and experiment. However, such an agreement does not increase our knowledge of the real system. It just proves that even a simple model of BZ-reaction can be used for a qualitative modeling of chemical memory.

Acknowledgements

The research was supported by the NEUNEU project sponsored by the European Community within FP7-ICT-2009-4 ICT-4-8.3 – FET Proactive 3: Biochemistry-based Information Technology (CHEM-IT) program. The financial support of the Foundation for Polish Science (MPD/2009/1/styp14) to KG is gratefully acknowledged. The final stage of the work was supported by the Polish National Science Centre grant UMO-2014/15/B/ST4/04954.

References

1 R. P. Feynman, *Feynman Lectures on Computation*, Addison-Wesley Longman Publishing Co., Inc., Boston, MA, USA, 1998.
2 H. Iwai, *Solid-State Electron.*, 2015, **112**, 56–67.
3 G. E. Moore, *Proc. IEEE*, 1998, **86**, 82–85.
4 V. V. Zhirnov, R. K. Cavin, J. A. Hutchby and G. I. Bourianoff, *Proc. IEEE*, 2003, **91**, 1934–1939.
5 T. Gramss, S. Bornholdt, M. Gross, M. Mitchell and T. Pellizzari, *Non-Standard Computation: Molecular Computation – Cellular Automata – Evolutionary Algorithms – Quantum Computers*, Wiley-VCH Verlag GmbH & Co. KGaA, 2005.
6 E. Katz, *Biomolecular information processing: from logic systems to smart sensors and actuators*, John Wiley & Sons, 2012.
7 E. Katz, *Molecular and supramolecular information processing: from molecular switches to logic systems*, John Wiley & Sons, 2013.
8 A. Adamatzky, *Philos. Trans. R. Soc., A*, 2015, **373**, 20140216.
9 A. Adamatzky, B. D. L. Costello and T. Asai, *Reaction-Diffusion Computers*, Elsevier Science Inc., New York, NY, USA, 2005.
10 J. Gorecki and J. N. Gorecka, in *Computing in Geometrical Constrained Excitable Chemical Systems*, ed. A. R. Meyers, Springer New York, New York, NY, 2009, pp. 1352–1376.
11 A. N. Zaikin and A. M. Zhabotinsky, *Nature*, 1970, **225**, 535–537.
12 K. Yoshikawa, I. Motoike, T. Ichino, T. Yamaguchi, Y. Igarashi, J. Gorecki and J. N. Gorecka, *Int. J. Unconv. Comput.*, 2009, **5**, 3–37.
13 V. K. Vanag and I. R. Epstein, *Proc. Natl. Acad. Sci. U. S. A.*, 2003, **100**, 14635–14638.
14 I. S. Proskurkin, A. I. Lavrova and V. K. Vanag, *Chaos*, 2015, **25**, 064601.
15 V. K. Vanag, P. S. Smelov and V. V. Klinshov, *Phys. Chem. Chem. Phys.*, 2016, **18**, 5509–5520.
16 J. Szymanski, J. Gorecka, Y. Igarashi, K. Gizynski, J. Gorecki, K. Zauner and M. D. Planque, *Int. J. Unconv. Comput.*, 2011, **7**, 185–200.
17 NeuNeu: artificial wet neuronal networks from compartmentalised excitable chemical media project, http://neu-n.eu/.
18 J. Holley, I. Jahan, B. De Lacy Costello, L. Bull and A. Adamatzky, *Phys. Rev. E: Stat., Nonlinear, Soft Matter Phys.*, 2011, **84**, 056110.
19 S. Thutupalli, S. Herminghaus and R. Seemann, *Soft Matter*, 2011, **7**, 1312–1320.
20 S. Thutupalli and S. Herminghaus, *Eur. Phys. J. E: Soft Matter Biol. Phys.*, 2013, **36**, 1–10.
21 J. Gorecki, K. Gizynski, J. Guzowski, J. Gorecka, P. Garstecki, G. Gruenert and P. Dittrich, *Philos. Trans. R. Soc., A*, 2015, **373**, 20140219.
22 J. Guzowski, K. Gizynski, J. Gorecki and P. Garstecki, *Lab Chip*, 2016, **16**, 764–772.
23 J. Delgado, N. Li, M. Leda, H. O. Gonzalez-Ochoa, S. Fraden and I. R. Epstein, *Soft Matter*, 2011, **7**, 3155–3167.
24 N. Tompkins, N. Li, C. Girabawe, M. Heymann, G. B. Ermentrout, I. R. Epstein and S. Fraden, *Proc. Natl. Acad. Sci. U. S. A.*, 2014, **111**, 4397–4402.
25 G. Gruenert, J. Szymanski, J. Holley, G. Escuela, A. Diem, B. Ibrahim, A. Adamatzky, J. Gorecki and P. Dittrich, *Int. J. Unconv. Comput.*, 2013, **9**, 237–266.
26 K. Gizynski, G. Gruenert, P. Dittrich and J. Gorecki, *Evol. Comput*, 2016, DOI: 10.1162/EVCO_a_00197.
27 I. N. Motoike, K. Yoshikawa, Y. Iguchi and S. Nakata, *Phys. Rev. E: Stat., Nonlinear, Soft Matter Phys.*, 2001, **63**, 036220.
28 A. Kaminaga, V. K. Vanag and I. R. Epstein, *Angew. Chem., Int. Ed.*, 2006, **45**, 3087–3089.
29 J. Gorecki and J. Gorecka, *Mathematical Approach to Nonlinear Phenomena; Modeling, Analysis and Simulations, GAKUTO International Series, Mathematical Sciences and Applications*, 2005, **23**, 73–90.
30 F. Muzika and I. Schreiber, *J. Chem. Phys.*, 2013, **139**, 164108.
31 F. Muzika, L. Schreiberová and I. Schreiber, *RSC Adv.*, 2014, **4**, 56165–56173.
32 F. Muzika, L. Schreiberová and I. Schreiber, *React. Kinet., Mech. Catal.*, 2016, **118**, 99–114.
33 M. I. Kohira, N. Magome, H. Kitahata and K. Yoshikawa, *Am. J. Phys.*, 2007, **75**, 893–895.
34 M. I. Kohira, N. Magome, S. Mouri, H. Kitahata and K. Yoshikawa, *Int. J. Unconv. Comput.*, 2009, **5**, 103–111.
35 M. I. Kohira, H. Kitahata, N. Magome and K. Yoshikawa, *Phys. Rev. E: Stat., Nonlinear, Soft Matter Phys.*, 2012, **85**, 026204.
36 W. Rasband, *ImageJ*, U. S. National Institutes of Health, Bethesda, Maryland, USA, 1997–2016, http://imagej.nih.gov/ij/.
37 V. K. Vanag, A. M. Zhabotinsky and I. R. Epstein, *J. Phys. Chem. A*, 2000, **104**, 8207–8215.

38 L. Kuhnert, K. I. Agladze and V. I. Krinsky, *Nature*, 1989, **337**, 244–247.
39 S. Kadar, T. Amemiya and K. Showalter, *J. Phys. Chem. A*, 1997, **101**, 8200–8206.
40 M. Toiya, H. O. Gonzalez-Ochoa, V. K. Vanag, S. Fraden and I. R. Epstein, *J. Phys. Chem. Lett.*, 2010, **1**, 1241–1246.
41 J. Gorecki, J. N. Gorecka and A. Adamatzky, *Phys. Rev. E: Stat., Nonlinear, Soft Matter Phys.*, 2014, **89**, 042910.
42 O. Steinbock and S. C. Mueller, *J. Phys. Chem. A*, 1998, **102**, 6485–6490.
43 A. Toth, V. Gaspar and K. Showalter, *J. Phys. Chem.*, 1994, **98**, 522–531.
44 R. Bradbury and M. Nagao, *Soft Matter*, 2016, **12**, 9383–9390.
45 J. M. Davidenko, A. V. Pertsov, R. Salomonsz, W. Baxter and J. Jalife, *Nature*, 1992, **355**, 349–351.
46 V. K. Vanag and I. R. Epstein, *Phys. Rev. E: Stat., Nonlinear, Soft Matter Phys.*, 2011, **84**, 066209.
47 J. Gorecki, J. Szymanski and J. N. Gorecka, *J. Phys. Chem. A*, 2011, **115**, 8855–8859.